J. Wind Eng. Ind. Aerodyn. 98 (2010) 712–723

Contents lists available at ScienceDirect

Journal of Wind Engineering and Industrial Aerodynamics

journal homepage: www.elsevier.com/locate/jweia

Gust alleviation using rapidly deployed trailing-edge flaps

M. Frederick [a,*], E.C. Kerrigan [a,b], J.M.R. Graham [a]

[a] Department of Aeronautics, Imperial College London, London SW7 2AZ, UK
[b] Department of Electrical and Electronic Engineering, Imperial College London, London SW7 2AZ, UK

ARTICLE INFO

Article history:
Received 1 October 2009
Received in revised form
4 May 2010
Accepted 4 June 2010
Available online 17 July 2010

Keywords:
Active
Load
Control
Wind
Gust alleviation
Small
Trailing-edge flap
Microtab

ABSTRACT

This paper presents the results of a numerical and experimental investigation into the use of a small, rapidly actuated, actively controlled trailing-edge flap (4% chord) to alleviate the unsteady loading experienced by wind turbine blades due to atmospheric turbulence and the atmospheric boundary layer.

The computational investigation demonstrated that the rejection of realistic flow disturbances should be feasible with the use of load measurements on the blade and the feedback control of a small flap. The experimental prototype subsequently successfully rejected intentionally introduced flow disturbances from the vortex street of a square block located upstream of a sting-mounted, strain-gauged wing fitted with flap. This application of control provided a very significant reduction in the unsteady loading experienced ($\sim$81% of C_{LRMS}).

The findings show the potential of this method of load control for the rejection of unsteady aerodynamic loading by the sole use of load measurements from the wing for simple feedback control (PID/LQG).

1. Introduction

Streamlined lifting surfaces, such as wind turbine blades, helicopter blades or aeroplane wings are subjected to unsteady loadings due to atmospheric turbulence. In addition, for large wind turbine blades, their relative size compared with the thickness of the atmospheric boundary layer means that they are subjected to a cyclic loading over each rotation due to the mean wind shear. These unsteady flapwise loadings cause fatigue over the lifetime of a typical wind turbine blade. A means of maintaining a steady or prescribed blade loading is therefore desirable for reducing fatigue, but also for reducing the extent of periodic vibrations such as those experienced by helicopters. Currently, some wind turbines vary the pitch of the entire blade by rotation. However, this method is too slow to be used to attenuate the effect of atmospheric turbulence. A conventional solution using a controlled flap deflection would comprise moving a large flap through a small angle to effect a change in the lift on the blade (Hassan et al., 2005). A small trailing-edge flap can be deployed at a much higher rate because of its smaller moment of inertia, which suggests that it could be used to counter both shorter gusts, as well as acting much more rapidly and effectively.

Flaps of the small sizes investigated in this work (<5% chord) at very high flap incidence ($\sim$45–90°) have been used statically for several decades on aerofoils to increase the lift generated and their aerodynamic characteristics are well known and understood (Giguère et al., 1995; Jeffrey et al., 2000; Storms and Jang, 1994; Troolin et al., 2006). The design of these Gurney-type flaps consists of a small flap, fixed at the trailing edge of the aerofoil. The flap is typically deployed statically on the lower surface with the flap angle $\delta=90^\circ$. Their typical aerodynamic properties can be found, for example, in Jeffrey et al. (2000), where the lift and drag coefficients, C_L and C_D respectively, are defined in Nomenclature.

Despite their small size, relative to the aerofoil chord, static Gurney flaps can effect large changes in the lift generated on an aerofoil. A schematic is shown in Fig. 1(a). Thus, a device of this type, when hinged at the trailing-edge and deployed dynamically between $\pm 90^\circ$ (i.e. on either the upper or lower surface), as considered in this work, is potentially capable of rejecting the expected levels of unsteady loading generated on wind turbine blades by atmospheric turbulence. A schematic of such a device is shown in Fig. 1(b). For a thorough overview of the history and application of static (in contrast to the dynamically deployed devices considered in this work), Gurney-type devices, the interested reader is referred to Wang et al. (2008). The deployment of tabs normal to the surface of the aerofoil slightly forward of the trailing-edge has also been investigated (for example van Dam et al., 1999) and they have been found to have similar mean aerodynamic properties as those located at the trailing-edge.

The focus of the present work is on alleviating the unsteady loading on blades due to any aerodynamic disturbance, such as atmospheric turbulence or upstream turbine wakes, passing across the wind turbine. For wind turbines, such disturbances

* Corresponding author.
E-mail address: mark.frederick@hotmail.fr (M. Frederick).

0167-6105/$ - see front matter © 2010 Published by Elsevier Ltd.
doi:10.1016/j.jweia.2010.06.005

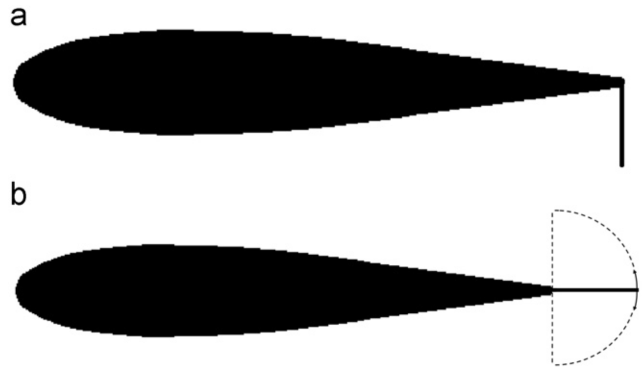

Fig. 1. Static gurney flap (a) and dynamically deployed trailing-edge flap (b).

can have reduced frequencies up to the order of $k=1$ (Leishman, 2002) where $k=\omega c/2U$ and where c is the aerofoil chord, U the relative flow velocity and ω the characteristic frequency of the flow disturbance (rad s^{-1}). Near the tips of wind turbine blades at the very highest operating wind speeds, the onset of compressibility effects may also appear marginally ($M\sim0.3$), although operation under such flow conditions was not considered in this current work.

The power spectrum of wind speed shows two peaks: the first, with periods of days; the second, with periods of seconds, the latter being the peak of interest in the current work. This spectrum is reproduced in Harris (2008) but is originally due to van der Hoven (1957). The peak of interest occurs around 1.2 s which, for the Vestas^{TM} V90-3.0 wind turbine is equivalent to around $T^*=90$ near the blade tips at the rated wind speed (14 m s^{-1}). T^* is the non-dimensional period associated with the non-dimensional time t^*, which in turn is defined in terms of the actual time t (s), the flow velocity U (m s^{-1}) and the aerofoil chord c (m): $t^*=Ut/c$. Under these conditions, the Reynolds number near the blade tips would be around 5×10^6.

Another important contribution to fatigue is the 1/rev cyclic loading experienced by wind turbine blades as they rotate through the atmospheric boundary layer. An approximate estimate of the size of the change in loading required can be calculated from the flapwise bending moment data taken by Schubert (1996) for a 48 m diameter rotor. Here, the measured bending moment is clearly dominated by a 1/rev oscillation. Assuming a tip-speed-ratio (TSR) of 7 and a NACA 63(3)-218 blade section, with the centre of lift of the blade acting at 3/4 span, an estimated C_L range is 0.9 ± 0.4. Measurements of the bending stress of a wind turbine located in mountainous and rough terrain by Tsuchiya and Inomata (1996) suggest that wind speed and stress amplitude are not (at least in hilly terrain) correlated as might be expected: large stresses were measured over the whole operating range of wind speeds. The frequency spectrum of measured stress contained peaks at 0.725, 1.450 and 2.225 Hz. Although details of the turbine are not given in the paper, it is a 300 kW turbine, which is typically around 30 m in diameter. Assuming a TSR of 7 and a rated wind speed of 12 m s^{-1}, these peak stresses would typically occur with non-dimensional periods of around $T^*=120$, 60 and 40 near the blade tips.

2. Numerical modelling

In this section a variety of controllers are tested on two inviscid models: the first, a high-order panel model (Section 2.1); the second, a low-order state-space model (Section 2.2). Inviscid models do not include the effects of separation and therefore substantially overpredict the lift generated by, for example, a flap deploying through a large angle. The justification for using such models in a problem involving separated flow is twofold: firstly, their potential for capturing the main dynamics of the physical system; secondly, their simplicity. Fig. 2 shows a comparison between the viscous computational fluid dynamics (CFD) simulation of a NACA 0012 aerofoil with a 1% chord flap deployed through 90° in $T^*=1$ performed by van Dam et al. (2007) and the inviscid state-space model developed and described in this section. The flap is deployed with a sinusoidal velocity described by

$$\begin{aligned}\dot{\delta}(t)&=\frac{\delta_{max}\pi}{2T_d}\sin\left(\frac{\pi t}{T_d}\right) & 0\le t\le T_d\\ \dot{\delta}(t)&=0 & t>T_d\end{aligned}\qquad(1)$$

where δ_{max} is the final flap angle (in this case 90°) and T_d is the period of the deployment. The inviscid state-space model result is normalised against the viscous result at $t^*=10$. After this normalisation, there is excellent agreement between these two results: the inviscid model effectively captures the dynamics of the system. Note that there is vortex shedding in the results by van Dam et al. (2007) after $t^*\sim0.8$: the mean values are shown at discrete points for comparison with the normalised state-space result.

2.1. High-order panel model

In this section, the development of a high-order panel model is described. The real system under investigation is a blade at low incidence mounted with a small, rapidly deployed trailing-edge flap shedding, for small flap deflection angles, a continuous vortex sheet from the trailing-edge of the flap. As a first approximation, it is reasonable to simplify and model this blade-flap system as a flat plate with attached moving flap using unsteady, incompressible, panel methods detailed in Katz and Plotkin (1991) with the addition of flap motion. In this type of model, the aerofoil and flap are broken up into a series of two-dimensional panels and a vortex placed at one-quarter distance along each panel. The collocation points are located at three-quarter distance along each panel, as shown in Fig. 3. The zero-flow normal boundary condition must be enforced at each collocation point for the system of panels with a no-slip condition applied at the blade surface.

In reality, the unsteady wake consists of the shedding of a continuous vortex sheet of length $\Delta S\approx\sqrt{U^2+W^2}\Delta t$ where U and W are the mean flow velocities in the x and z directions,

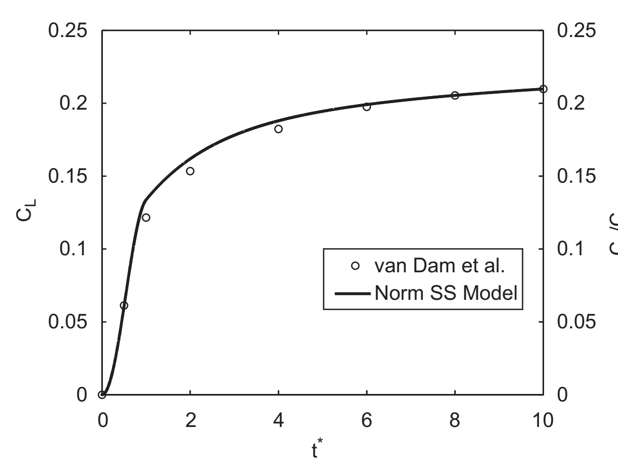

Fig. 2. Comparison between viscous numerical results (van Dam et al., 2007) and inviscid model.